Structure of an Engineered His_3Cys Zinc Binding Site in Human Carbonic Anhydrase II[†,‡]

Joseph A. Ippolito and David W. Christianson*

Department of Chemistry, University of Pennsylvania, Philadelphia, Pennsylvania 19104-6323

Received June 30, 1993[⊕]

ABSTRACT: X-ray crystallographic analysis of the Thr-199→Cys (T199C) variant of human carbonic anhydrase II reveals the first high-resolution structure of an engineered zinc coordination polyhedron in a metalloenzyme. In the wild-type enzyme, Thr-199 accepts a hydrogen bond from zinc-bound hydroxide; in the variant, the polypeptide backbone is sufficiently plastic to permit Cys-199 to displace hydroxide ion and coordinate to zinc with nearly perfect coordination stereochemistry. Importantly, the resulting His_3-Cys–Zn^{2+} motif binds zinc more tightly than the wild-type enzyme [Kiefer, L. L., Krebs, J. F., Paterno, S. A., & Fierke C. A. (1993) *Biochemistry* (preceding paper in this issue)]. This novel zinc coordination polyhedron is analogous to that postulated for matrix metalloproteinase zymogens such as prostromelysin, where a cysteine–zinc interaction is responsible for the inactivity of the zymogen. Intriguingly, Cys-199 of T199C CAII is displaced from zinc coordination by soaking crystals in high concentrations of acetazolamide. Hence, residual catalytic activity measured for this variant probably arises from an alternate conformer of Cys-199 which allows the catalytic nucleophile, hydroxide ion, to be activated by zinc coordination.

Carbonic anhydrase II (CAII)[1] is a prototypical zinc metalloenzyme that catalyzes the hydration of carbon dioxide (Silverman & Lindskog, 1988; Christianson, 1991). The three-dimensional structure of the human blood enzyme has been determined and refined at 1.54-Å resolution (Håkansson et al., 1992), and the structure of the recombinant wild-type protein is essentially identical (Alexander et al., 1991). Recent genetic–structural analyses of CAII focus on the catalytic importance of the active site hydrophobic pocket (Fierke et al., 1991; Alexander et al., 1991; Nair et al., 1991), as well as certain hydrophilic residues elsewhere in the enzyme active site (Krebs et al., 1991). Not only has this work been important for understanding the molecular details of catalysis but it has also provided the first glimpse of the compensatory "plasticity" (Perry et al., 1990) of the protein scaffolding. Subtle structural changes accompany amino acid substitutions in the polypeptide chain of CAII, and these structural changes propagate for several angstroms away from the point of mutation through the protein scaffolding (Alexander et al., 1991) or across the protein surface [mediated via solvent; see Krebs et al. (1991)]. For instance, the Ser-197→Cys-206 polypeptide loop is quite versatile in the plastic accommodation of amino acid substitutions in the CAII active site, and such plasticity can now be exploited in protein design experiments which focus on the adjacent metal binding site.

Here, the wild-type zinc coordination polyhedron of CAII (comprised of His-94, His-96, His-119, and hydroxide ion) has been altered by engineering a fourth protein ligand through residue 199, and the three-dimensional structure of the metalloenzyme variant has been determined by X-ray crystallographic methods to a resolution of 2.2 Å. In the wild-type enzyme, the hydroxyl group of Thr-199 accepts a hydrogen bond from zinc-bound hydroxide and donates a hydrogen bond to the ionized side chain of Glu-106. Thr-199 orients zinc-bound hydroxide for nucleophilic attack at substrate CO_2 (Merz, 1990), and the hydrogen bond stereochemistry for this interaction is optimal (Ippolito et al., 1990). However, the substitution Thr-199→Cys (T199C), which could potentially maintain the hydrogen bond with zinc-bound hydroxide, results in a 10^3-fold loss of CO_2 hydrase activity (Kiefer et al., 1993). The structure of T199C CAII reveals that the significant loss of catalytic activity arises from the displacement of zinc-bound hydroxide by the engineered Cys-199 thiolate group, an interaction which is facilitated by the structural plasticity of the Ser-197→Cys-206 polypeptide loop. Moreover, the residual activity measured for T199C CAII implies that there must be two conformations for the Cys-199 side chain, such that the enzyme is inactive when Cys-199 is coordinated to zinc (Cys_{bound} conformation), and the enzyme is active when Cys-199 is not coordinated to zinc ($Cys_{unbound}$ conformation). Importantly, we find that this conformational change is triggered by incubating the crystalline enzyme variant with a transition-state analogue inhibitor.

Protein engineering lessons learned by the modification of the structurally characterized zinc binding site of CAII serve as a reference for the design and construction of avid, *de novo* zinc binding sites in other protein scaffoldings which are more elusive to structural characterization. Some of these structurally uncharacterized protein metal binding sites are based on CAII as a template and include metalloantibodies (Iverson et al., 1990; Roberts et al., 1990), "minibodies" (Pessi et al., 1993), α-helical peptides (Ghadriri & Choi, 1990; Ruan et al., 1990), and α-helix bundles (Handel & DeGrado, 1990; Regan & Clarke, 1990). More recently, regulatory transition metal binding sites have been engineered in trypsin (Higaki et al., 1990) and glycogen phosphorylase (R. J. Fletterick, personal communication), and the structures of metal-bound enzyme variants have been determined by X-ray crystallographic methods (McGrath et al., 1993; R. J. Fletterick,

[†] Supported by the Office of Navel Research and the NIH. D.W.C. thanks the Alfred P. Sloan Foundation for a research fellowship and the Camille and Henry Dreyfus Foundation for a teacher–scholar award. J.A.I. is supported in part by NIH Training Grant GM08275.

[‡] The atomic coordinates of the refined models have been deposited in the Brookhaven Protein Data Bank (reference codes 1DCA and 1DCB) (Bernstein et al., 1977).

* Author to whom correspondence should be addressed.

[⊕] Abstract published in *Advance ACS Abstracts*, September 1, 1993.

[1] Abbreviations: CAII, human carbonic anhydrase II; T199C, Thr-199→Cys (threonine-199→cysteine); MMP, matrix metalloproteinase.

0006-2960/93/0432-9901$04.00/0

personal communication). Finally, the H94C variant of CAII yields a metal coordination polyhedron of His_2Cys, and the apoenzyme of this variant crystallizes in a new space group (Alexander et al., 1993). We note that general structure-assisted approaches toward the design and construction of transition metal binding sites in proteins have been recently reviewed (Higaki et al., 1992; Tainer et al., 1992).

MATERIALS AND METHODS

T199C CAII was the generous gift of Dr. C. A. Fierke. Crystals were prepared as described (Alexander et al., 1991) except that no methylmercury acetate was present in the crystallization solutions, and crystals of typical dimensions 0.2 mm × 0.4 mm × 0.6 mm appeared within 2 weeks at 4 °C. The enzyme variant formed crystals isomorphous with those of the wild-type enzyme and belonged to monoclinic space group $P2_1$ with typical unit cell parameters: a = 42.7 Å, b = 41.7 Å, c =73.0 Å, and β = 104.6°.

A crystal of T199C CAII was mounted and sealed in a 0.5-mm glass capillary along with a small portion of mother liquor. A Siemens X-100A multiwire area detector, mounted on a three-axis camera and equipped with Charles Supper double X-ray focusing mirrors, was used for X-ray data acquisition. A Rigaku RU-200 rotating anode X-ray generator operating at 45 kV/65 mA supplied Cu Kα radiation. All data were collected at room temperature by the oscillation method; the crystal-to-detector distance was set at 10 cm, and the detector swing angle was fixed at 20°. Data frames of 0.0833° oscillation about ω were collected, with exposure times of 60 s/frame, for total angular rotation ranges about ω of at least 80° per run. Two data sets for the enzyme were collected, and diffraction intensities were measured to a limiting resolution of 2.2 Å. Raw data frames were analyzed using the BUDDHA package (Durbin et al., 1986), reflections with $I < 2\sigma$ were discarded, and replicate and symmetry-related data were merged using PROTEIN (Steigmann, 1974). Data were also collected to 2.1-Å resolution from a crystal soaked for 1 week in 10 mM acetazolamide (a sulfonamide inhibitor). Pertinent data collection and reduction statistics for inhibitor-free and inhibitor-treated forms of T199C CAII are recorded in Table I.

The protein model of T199C CAII was refined against data in the 7.0–2.2-Å shell using PROLSQ (Hendrickson, 1985). The side chain of Cys-199 was not included in the protein model until the crystallographic R factor dropped below 0.20. During the course of refinement, structure factors obtained from corrected intensity data were used to generate difference electron density maps using Fourier coefficients $2|F_o| - |F_c|$ and $|F_o| - |F_c|$ with phases calculated from the structure of the in-progress model. Model building was performed with the graphics software FRODO (Jones, 1985) installed on an Evans and Sutherland PS390 interfaced with a VAXstation 3500. In the starting structure, it was evident that significant rearrangement of the Ser-197→Cys-206 polypeptide loop in the vicinity of Cys-199 had occurred, and this region was remodeled accordingly. After the crystallographic R factor dropped below 0.20, active site water molecules were added and refined. Residue conformations throughout the protein were examined during the course of refinement by using maps calculated with Fourier coefficients outlined above and phases derived from the in-progress atomic model—minimal adjustments of atomic positions were necessary. Refinement converged smoothly to a final crystallographic R factor of 0.182.

The model of acetazolamide-treated T199C CAII was built and refined by a protocol similar to that employed for the inhibitor-free structure. Although electron density maps revealed only noisy and discontinuous density corresponding to the inhibitor, these maps unambiguously indicated that the predominant conformer of Cys-199 was *not* coordinated to zinc. Therefore, for the purposes of refinement the atomic coordinates of a bound inhibitor were not refined, and the nonprotein zinc ligand was refined as a water molecule. Refinement of the inhibited enzyme structure against data in the 7.0–2.1-Å range yielded a final crystallographic R factor of 0.182. Pertinent refinement statistics of inhibitor-free and inhibitor-treated forms of T199C CAII are recorded in Table I.

Table I: Data Collection and Refinement Statistics

	T199C CAII	acetazolamide complex
no. of crystals	1	1
no. of measured reflections	14756	23067
no. of unique reflections	10345	11766
max resolution (Å)	2.2	2.1
$R_{merge}(I)^a$	0.056	0.084
no. of water molecules in final cycle of refinement	100	93
no. of reflections used in refinement (7.0 Å – max resolution)	8938	11048
completeness of data (%)	72.3	77.6
parameter/observation ratio	0.953	0.768
crystallographic R factor[b]	0.182	0.182
RMS deviation from ideal bond lengths (Å)	0.014	0.015
target value	0.030	0.030
RMS deviation from ideal bond angle lengths (Å)	0.027	0.033
target value	0.040	0.050
RMS deviation from ideal planarity (Å)	0.009	0.012
target value	0.025	0.030
RMS deviation from ideal chirality (Å^3)	0.085	0.079
target value	0.150	0.150

[a] R_{merge} calculated for replicate reflections: $R = \sum|I_{hi} - \langle I_h\rangle|/\sum\langle I_h\rangle$; I_{hi} = intensity measure for reflection h in data set i; $\langle I_h\rangle$ = average intensity for reflection h calculated from replicate data. [b] Crystallographic R factor: $R = \sum||F_o| - |F_c||/\sum|F_o|$; $|F_o|$ and $|F_c|$ are the observed and calculated structure factors, respectively.

For each refined structure, a difference electron density map calculated with Fourier coefficients $|F_o| - |F_c|$ and phases derived from the coordinates to the final model revealed that the highest peaks in the vicinity of the active site were less than 3.5σ. Additionally, the RMS error in atomic positions for each structure was estimated to be ca. 0.2 Å on the basis of relationships derived by Luzzati (1952).

RESULTS AND DISCUSSION

Structural Basis of Enhanced Protein–Zinc Affinity. A difference electron density map of T199C CAII reveals that the thiolate side chain of Cys-199 displaces zinc-bound hydroxide and coordinates to zinc (Figure 1). The active site zinc ion is additionally coordinated by His-94, His-96, and His-119 in tetrahedral fashion; zinc–ligand distances are recorded in Table II, and zinc–ligand angles are recorded in Table III. Importantly, this is the first high-resolution structure of a protein–zinc complex involving three histidine residues and one cysteine thiolate. We note that the 3.5-Å resolution structure of β-lactamase II from *Bacillus cereus* contains a putative His_3Cys–Cd^{2+} complex, but the structural details of metal coordination at this resolution are not well-defined (Sutton et al., 1987).

Conformational analysis of the engineered metal binding site reveals the structural features that contribute to enhanced protein–zinc affinity measured by Kiefer et al. (1993). Torsion angle χ_1 of Cys-199 is 50°, which is in accord with energetically favorable values tabulated by Ponder and Richards (1987).

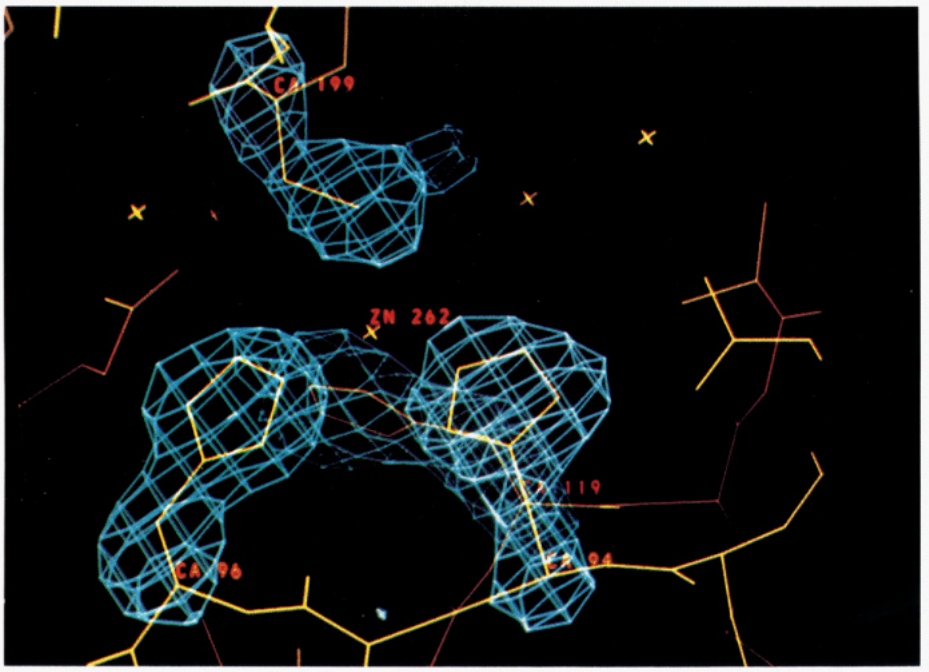

FIGURE 1: Difference electron density map (contoured at 3σ) of T199C CAII. His-94, His-96, His-119, and Cys-199 were omitted from the structure factor calculation. Refined atomic coordinates are superimposed, and zinc and its ligands are indicated. This is the catalytically inhibited, Cys_{bound} conformation of the regulatory cysteine switch.

Table II: Zinc–Ligand Distances (Å)

ligand	wild-type CAII	T199C CAII	acetazolamide complex
His-94 Nε2	2.3	2.2	2.2
His-96 Nε2	2.1	2.1	2.1
His-119 Nδ1	2.2	2.1	2.0
nonprotein ligand	2.4		2.4
Cys-199 Sγ		2.4	

Table III: Ligand–Zinc–Ligand Angles (deg)

ligand 1	ligand	wild-type CAII	T199C CAII	acetazolamide complex
His-94 Nε2	His-96 Nε2	108	102	107
	His-119 Nδ1	110	112	113
	nonprotein ligand	105		104
	Cys-199 Sγ		110	
His-96 Nε2	His-119 Nδ1	91	96	107
	nonprotein ligand	130		103
	Cys-199 Sγ		107	
His-119 Nδ1	nonprotein ligand	111		122
	Cys-199 Sγ		127	

Additionally, Cys-199 exhibits a C–C–$S^- \rightarrow Zn^{2+}$ torsion angle of 179°, and this value is optimal for cysteine–metal ion interactions (Chakrabarti, 1989). Therefore, the engineered linkage between Cys-199 and zinc reflects the optimal conformational properties to which thiolate–zinc interactions have evolved in naturally occurring metalloproteins. We note that Cys-199 is not stabilized by hydrogen bond donor interactions with protein or ordered solvent molecules, e.g., as observed in other metalloproteins (Adman et al., 1975). Such interactions may enhance the stability of the protein–metal complex as well as the chemical function of the bound metal ion (Ippolito et al., 1990; Gregoret et al., 1991).

The overall structure of T199C CAII is essentially identical to that of the wild-type enzyme, and the least-squares superposition of both structures yields an RMS deviation of 0.2 Å for Cα atoms. The most prominent structural difference between the two structures involves the Ser-197→Cys-206 loop, which endures a significant structural change in order to facilitate Cys-199 coordination to zinc (Figure 2). As mentioned in the introduction, previous X-ray crystallographic studies show that this loop is quite versatile in the plastic accommodation of amino acid substitutions in the CAII active site (Alexander et al., 1991).

Catalysis Requires a Conformational Change of Cys-199. It is difficult at first to reconcile activity measurements made on T199C CAII in solution with the structure of the enzyme variant in the crystal showing Cys-199 in the zinc-bound conformation (Cys_{bound}), since Kiefer et al. (1993) provide compelling evidence that the variant enzyme catalyzes CO_2 hydration, albeit 10^3-fold slower, by the same chemical mechanism as that employed by the wild-type enzyme (i.e., via a zinc hydroxide nucleophile). However, an alternate, low-occupancy conformation of Cys-199 not bound to zinc (i.e., the $Cys_{unbound}$ conformation) would allow for zinc hydroxide coordination and thereby would yield an active enzyme. This possibility would reconcile solution and crystal data: the small population of enzyme molecules with $Cys_{unbound}$ conformers would be responsible for the activity measured for the entire population of $Cys_{unbound}$ and Cys_{bound} conformers. For instance, since CO_2 hydrase activity is diminished by 10^3-fold (Kiefer et al., 1993), the population of $Cys_{unbound}$ conformers would be 0.1% if the Cys-$199_{unbound}$ variant exhibits activity comparable to that of the wild-type enzyme. If the Cys-$199_{unbound}$ variant exhibits 10–100-fold diminished activity relative to that of the wild-type enzyme (a more likely consequence), then the population of Cys-$199_{unbound}$ conformers in the crystal would range from 1% to 10%—such small conformer populations would not be interpretable in electron density maps of the crystalline enzyme variant.

In order to observe the structure of a Cys-$199_{unbound}$ conformer, we have determined the crystal structure of T199C CAII incubated with a buffer solution containing 10 mM transition-state analogue inhibitor, acetazolamide. In the native blood enzyme, the ionized sulfonamide nitrogen of acetazolamide coordinates to the active site zinc ion and simultaneously donates a hydrogen bond to the side chain of Thr-199 (Vidgren et al., 1990). In T199C CAII, acetazolamide binding is disordered. However, although electron density for the inhibitor is not readily interpretable (the

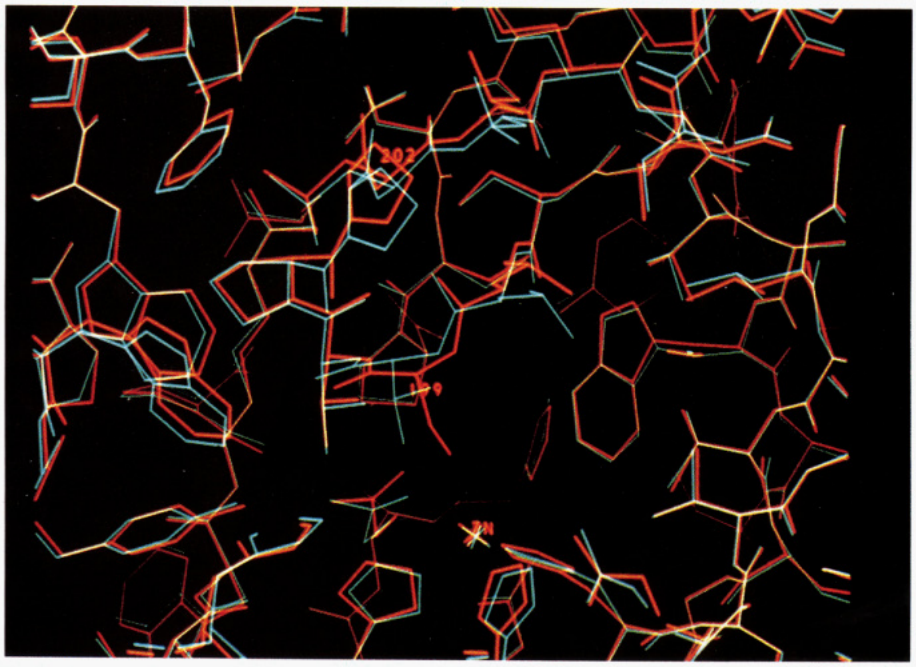

FIGURE 2: Least-squares superposition of wild-type and T199C CAIIs (blue and red, respectively). Zn^{2+}, Pro-202, and residue 199 are indicated.

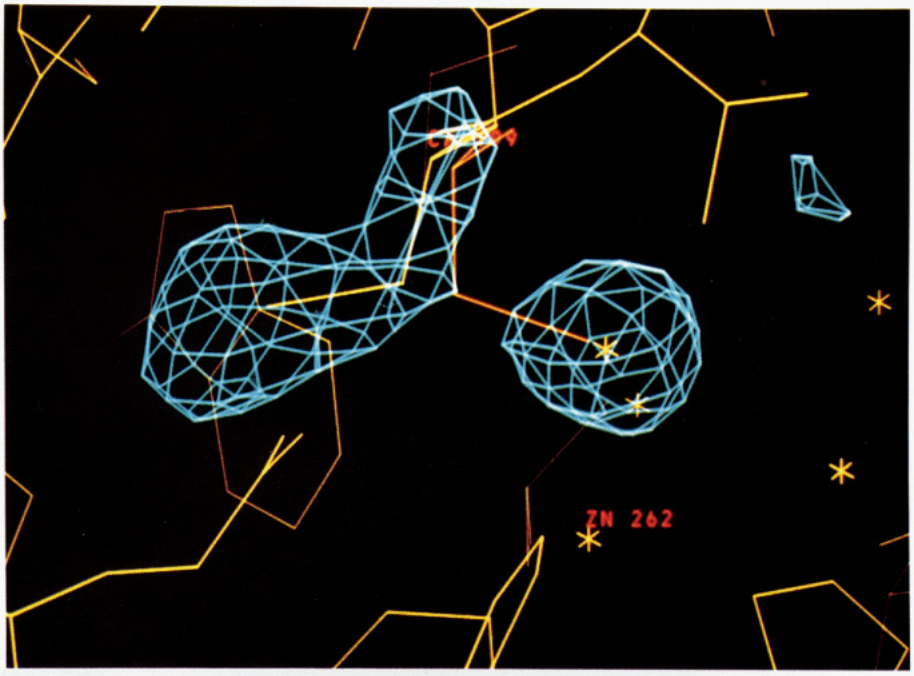

FIGURE 3: Difference electron density map (contoured at 3σ) of the T199C CAII–acetazolamide complex. Cys-199 and the nonprotein zinc ligand were omitted from the structure factor calculation. Refined atomic coordinates are superimposed (yellow), and Cys-199 and zinc are indicated. Here, Cys-199 is in the catalytically active, $Cys_{unbound}$ conformation. The 11σ peak corresponding to the nonprotein zinc ligand is either the disordered sulfonamide group of acetazolamide or a partially occupied Cys_{bound} conformer (superimposed, red). Electron density between this peak and Cys-199 becomes connected when the map is contoured at the relatively low level of 2σ.

strongest signal is an 11σ peak above the zinc ion), the electron density map in Figure 3 clearly shows that Cys-199 rotates 150° about χ_1 to the $Cys_{unbound}$ conformation in order to accommodate the nonprotein zinc ligand. Given that acetazolamide is presumed to be a transition-state analogue for the CO_2 hydrase reaction, we conclude that a comparable structural change of Cys-199 may equilibrate Cys_{bound} and $Cys_{unbound}$ conformers in order to accommodate the actual catalytic transition state.

The electron density corresponding to the nonprotein zinc ligand is centered 2.4 Å from the metal ion and probably corresponds to disordered inhibitor and/or a partially occupied Cys_{bound} conformer [this density was refined as a solvent molecule since it was not confidently interpretable as bound inhibitor; furthermore, due to lack of connectivity with the electron density of Cys-199 (except at the relatively low level of 2σ), we did not refine Cys_{bound} and $Cys_{unbound}$ confomers simultaneously]. The distance between the sulfur atom of $Cys_{unbound}$ and the nonprotein zinc ligand is 4.3 Å, which is too long to reflect a hydrogen bond interaction. Interestingly, this feature may suggest that a hydrogen bond interaction is not absolutely required for the catalytic activity of zinc-bound hydroxide, *if* the same $Cys_{unbound}$ conformer characterizes the catalytically active state of T199C CAII. We note that, in the structure of inhibitor-free T199C CAII, an additional water molecule engages Glu-106 in a poorly oriented hydrogen

bond, and this water molecule is in a location near that occupied by the Cys-199 sulfur in the $Cys_{unbound}$ conformation. It is possible that a partially occupied $Cys_{unbound}$ conformer contributes to the corresponding 9σ peak.

As it affects the function of zinc in T199C CAII, the operation of Cys-199 as a reversible metal ligand is markedly different from that of the regulatory cysteine side chain engineered into the active site of staphylococcal nuclease by Corey and Schultz (1989): here, the addition of mercuric or cuprous salts results in enzyme inactivation by steric blockage of substrate binding by the bound metal ion (activity is restored by the addition of chelating agents). In T199C CAII, the bound metal ion itself is an integral participant in catalysis, and the activity of the metal ion is governed by the conformation of Cys-199: the enzyme is inactive when Cys-199 coordinates to zinc ($Cys_{unbound}$), and the enzyme is active when Cys-199 is not coordinated to zinc ($Cys_{unbound}$). If the conformation and metal-binding behavior of Cys-199 can be altered at will, a reversible cysteine switch that regulates catalytic activity will result.

CONCLUSIONS

The X-ray crystallographic study of T199C CAII reveals the first example of an engineered cysteine–zinc interaction in a metalloprotein, and analysis of the variant protein structure reveals the conformational features which contribute to enhanced protein–metal affinity measured by Kiefer et al. (1993). Moreover, conformational changes of Cys-199 between zinc-bound and zinc-unbound states account for catalytically inactive and catalytically active forms, respectively, of the CAII variant. Given that the coordination of Cys-199 to zinc is displaceable by treating the crystalline enzyme variant with a buffer solution containing a transition-state analogue inhibitor, we conclude that Cys-199 is a reversible inhibitory element in the T199C CAII active site similar in spirit to cysteine switches which regulate the proenzyme forms of matrix metalloproteinases (MMP) such as prostromelysin (Van Wart et al., 1990; Salowe et al., 1992; Holz et al., 1992).

In MMPs, activation of the proenzyme is achieved by the cleavage of an 80 amino acid fragment from the amino terminus. Since the cysteine zinc ligand of a MMP proenzyme is contained in this amino-terminal fragment, the cleavage and dissociation of this fragment result in a vacant coordination site on zinc which is then occupied by water, the catalytic nucleophile. Given that recent EXAFS data are consistent with a zinc coordination polyhedron of His_3Cys in prostromelysin (Holz et al., 1992), it is intriguing to consider that the cysteine–zinc ligand of prostromelysin may itself be displaceable from the active site zinc ion by inhibitors (analogous to the behavior of Cys-199 in T199C CAII). Therefore, T199C CAII may serve as a useful model of the prostromelysin metal site, and the conformational behavior of zinc-coordinated cysteine residues may be a useful consideration in the design of MMP inhibitors.

ACKNOWLEDGMENT

We thank C. Fierke, R. Galardy, and S. Nair for helpul discussions.

REFERENCES

Adman, E., Watenpaugh, K. D., & Jensen, L. H. (1975) *Proc. Natl. Acad. Sci. U.S.A. 72*, 4854–4858.

Alexander, R. S., Nair, S. K., & Christianson, D. W. (1991) *Biochemistry 30*, 11064–11072.

Alexander, R. S., Kiefer, L. L., Fierke, C. A., & Christianson, D. W. (1993) *Biochemistry 32*, 1510–1518.

Bernstein, F. C., Koetzle, T. F., Williams, G. J. B., Meyer, E. F., Brice, M. D., Rodgers, J. R., Kennard, O., Shimanouchi, T., & Tasumi, M. (1977) *J. Mol. Biol. 112*, 535–542.

Chakrabarti, P. (1989) *Biochemistry 28*, 6081–6085.

Christianson, D. W. (1991) *Adv. Protein Chem. 42*, 281–355.

Corey, D. R., & Schultz, P. G. (1989) *J. Biol. Chem. 264*, 3666–3669.

Durbin, R. M., Burns, R., Moulai, J., Metcalf, P., Freymann, D., Blum, M., Anderson, J. E., Harrison, S. C., & Wiley, D. C. (1986) *Science 232*, 1127–1132.

Fierke, C. A., Calderone, T. L., & Krebs, J. F. (1991) *Biochemistry 30*, 11054–11063.

Ghadiri, M. R., & Choi, C. (1990) *J. Am. Chem. Soc. 112*, 1630–1632.

Gregoret, L. M., Rader, S. D., Fletterick, R. J., & Cohen, F. E. (1991) *Proteins: Struct., Funct., Genet. 9*, 99–107.

Håkansson, K., Carlsson, M., Svensson, L. A., & Liljas, A. (1992) *J. Mol. Biol. 227*, 1192–1204.

Handel, T., & DeGrado, W. F. (1990) *J. Am. Chem. Soc. 112*, 6710–6711.

Hendrickson, W. A. (1985) *Methods Enzymol. 115*, 252–270.

Higaki, J. N., Haymore, B. L., Chen, S., Fletterick, R. J., & Craik, C. S. (1990) *Biochemistry 29*, 8582–8586.

Higaki, J. N., Fletterick, R. J., & Craik, C. S. (1992) *Trends Biochem. Sci. 17*, 100–104.

Holz, R. C., Salowe, S. P., Smith, C. K., Cuca, G. C., & Que, L. (1992) *J. Am. Chem. Soc. 114*, 9611–9614.

Ippolito, J. A., Alexander, R. S., & Christianson, D. W. (1990) *J. Mol. Biol. 215*, 457–471.

Iverson, B. L., Iverson, S. A., Roberts, V. A., Getzoff, E. D., Tainer, J. A., Benkovic, S. J., & Lerner, R. A. (1990) *Science 249*, 659–662.

Jones, T. A. (1985) *Methods Enzymol. 115*, 157–171.

Kiefer, L. L., Krebs, J. F., Paterno, S. A., & Fierke, C. A. (1993) *Biochemistry* (preceding paper in this issue).

Krebs, J. F., Fierke, C. A., Alexander, R. S. & Christianson, D. W. (1991) *Biochemistry 30*, 9153–9160.

Luzatti, P. V. (1952) *Acta Crystallogr. 5*, 802–810.

McGrath, M. E., Haymore, B. L., Summers, N. L., Craik, C. S., & Fletterick, R. J. (1993) *Biochemistry 32*, 1914–1919.

Merz, K. M. (1990) *J. Mol. Biol. 214*, 799–802.

Nair, S. K., Calderone, T. L., Christianson, D. W., & Fierke, C. A. (1991) *J. Biol. Chem. 266*, 17320–17325.

Perry, K. M., Fauman, E. B., Finer-Moore, J. S., Montfort, W. R., Maley, G. F., Maley, F., & Stroud, R. M. (1990) *Proteins: Struct., Funct., Genet. 8*, 315–333.

Pessi, A., Bianchi, E., Crameri, A., Venturini, S., Tramontano, A., & Sollazzo, M. (1993) *Nature 362*, 367–369.

Ponder, J. W., & Richards, F. M. (1987) *J. Mol. Biol. 193*, 775–791.

Regan, L., & Clarke, N. D. (1990) *Biochemistry 29*, 10878–10883.

Roberts, V. A., Iverson, B. L., Iverson, S. A., Benkovic, S. J., Lerner, R. A., Getzoff, E. D., & Tainer, J. A. (1990) *Proc. Natl. Acad. Sci. U.S.A. 87*, 6654–6658.

Ruan, F., Chen, Y., & Hopkins, P. B. (1990) *J. Am. Chem. Soc. 112*, 9403–9404.

Salowe, S. P., Marcy, A. I., Cuca, G. C., Smith, C. K., Kopka, I. E., Hagmann, W. K., & Hermes, J. D. (1992) *Biochemistry 31*, 4535–4540.

Silverman, D. N., & Lindskog, S. (1988) *Acc. Chem. Res. 21*, 30–36.

Steigemann, W. (1974) Ph.D. Thesis, Max-Planck-Institut für Biochemie, Germany.

Sutton, B. J., Artymiuk, P. J., Cordero-Borboa, A. E., Little, C., Phillips, D. C., & Waley, S. G. (1987) *Biochem. J. 248*, 181–188.

Tainer, J. A., Roberts, V. A., & Getzoff, E. D. (1992) *Curr. Opin. Biotechnol. 3*, 378–387.

Van Wart, H. E., & Birkedal-Hansen, H. (1990) *Proc. Natl. Acad. Sci. U.S.A. 87*, 5578–5582.

Vidgren, J., Liljas, A., & Walker, N. P. C. (1990) *Int. J. Biol. Macromol. 12*, 342–344.